Indian Journal of Radio & Space Physics
Vol. 36, October 2007, pp. 369-374

Scintillation and depolarisation models for satellite communications in the 20-50 GHz band

Danielle Vanhoenacker-Janvier[1], Claude Oestges[1] & Antonio Martellucci[2]

[1]Microwave Laboratory, Université catholique de Louvain, Louvain-la-Neuve, Belgium

[2]TOS-EEP, ESA, ESTEC, Keplerlaan 1, PB 299, NL-2200 AG Noordwijk, The Netherlands

Email: vanhoenacker@emic.ucl.ac.be

Received 19 June 2007; accepted 14 September 2007

This paper presents improved methods for the prediction of cumulative distribution of scintillation variance, using radiosonde data. This method has the advantage of being usable all around the world and its accuracy is improved with respect to classical methods based only on ground measured data. The second part presents a two-layer depolarisation model separating rain and ice effects for better scalability.

Keywords: Tropospheric scintillation, Satellite communications, Depolarisation
PACS No.: 84.40. Ua

1 Introduction

With the rapid expansion in demand for new and global broadband communications services there is a need to develop the 20/30 and 40/50 GHz frequency bands, as well as prediction models accurate all around the world. Propagation through the Earth's atmosphere has a major impact on system design, and the various propagation effects increase in importance compared with lower frequency bands, requiring a high degree of accuracy and comprehensiveness in their prediction. In addition to attenuation phenomena induced by atmospheric gases, clouds and precipitation, tropospheric scintillation must be carefully considered in planning earth-space links designed to operate at high frequency bands or low elevation angles: the dynamics of scintillation is important for the implementation of fade mitigation techniques. The ITU-R[1] proposes a prediction method for the cumulative statistics of scintillation variance, based on ground temperature and humidity. As scintillation is due to turbulent layers in the troposphere, a model using temperature and humidity profiles should be more precise. This was the rationale of the use of radiosoundings for the prediction of tropospheric scintillation.

A second tropospheric effect, referred to as depolarisation, is in fact cross-talk between two orthogonally polarised channels, transmitted on the same path and in the same frequency band. This effect is mainly caused by hydrometeors such as raindrops and ice crystals. Due to their oblate or prolate spheroidal shapes, they can cause the propagation medium to become anisotropic and induce depolarisation.

This paper presents improved prediction methods for scintillation and depolarisation in the 20-50 GHz band.

2 Prediction of scintillation

The magnitude of tropospheric scintillation depends on the structure and intensity of refractive-index variations along the propagation path. Scintillation intensity increases with the microwave frequency of the transmitted signal and for smaller receiving antennas. Vertical profiles of atmospheric parameters (pressure, temperature and humidity) can be calculated all over the world using radiosonde data. The aim of the model presented in this paper is to predict scintillation all around the world, using radiosonde data. The classical radiosonde data from British Atmospheric Data Centre (BADC) are processed by interpolation, so that the data are available at equidistant height intervals of 50 m. From each radiosonde record, a corresponding profile of the mean value of refractive-index structure function parameter $< C_n^2 >$ is estimated following the probabilistic approach developed by UCL[2].

2.1 Calculation of C_n^2 profiles from low resolution radiosoundings

The vertical profiles of horizontal wind speed ($\bar{v}$), temperature (T) and specific humidity (q) have different scales of variation: a larger scale, of the

order of magnitude of 25-50 m, and a smaller scale of a few meters[3]. The smaller scale cannot be detected by standard radiosounding data, because usually the organization operating the radiosonde do not provide the data measured at all levels but only a subset. Such a small scale can be well represented by the high resolution radiosoundings (like the UK HiRES RAOBS database available at BADC) that retain all the valid original data. The fine structure is very strongly horizontally stratified[3]. The physical parameters used to describe the turbulent layer are, the shear parameter (vertical shear), the static stability, the Richardson number and the vertical derivative of the specific humidity.

Horizontal shear flows are dynamically unstable when $R_i < 0.25$ and generate turbulence in the layer. With sufficiently high resolution, the authors would be able to separate turbulent and non-turbulent layers and be able to calculate C_n^2 for each turbulent layer. The low resolution of the radiosonde with respect to the thickness of the turbulent layer obliges us to take a probabilistic approach, proposed by Warnock[4]. In a given slab of about 50 m, the rate of occurrence of turbulent layers and their distribution of thickness depends on the fine structure and the mean value of R_i. For example, if $R_i = 0.5$, the fraction of volume that is turbulent is about 0.5. The probability density functions of all the physical parameters (p_L for the outer scale, p_S for the shear parameter and p_N^2 for the static stability) have to be determined and finally, the average value of the refractive-index structure function parameter C_n^2 in the atmospheric layer at height z can be calculated by the relations:

$$\overline{C_n^2} = 2.8\, M_0^2\, \overline{R} \int_{L_{\min}}^{L_{\max}} L^{4/3} p_L dL \int p_S dS \int \left(N^2\right)^2 p_{N^2}^2 dN^2$$

$$M_0 = -\,77.6\,10^{-6}\,\frac{p}{gT}$$

$$\overline{R} = \left[\frac{q}{T} + 15500 \frac{\overline{q'}/T}{\overline{N^2}/g} \right]^2$$

where $L_{\min}$ and $L_{\max}$ are the minimum and maximum values of the outer scale of turbulence. This parameter is calculated versus height, using the potential temperature, humidity and wind speed profiles, as well as their first order derivative profiles. The extraction of $< C_n^2 >$ profile from one-month of radiosonde profile data collected at a meteorological station in Belgium revealed that the long-term statistical distribution of $< C_n^2 >$ indexed in height can be fairly approximated by a log-normal probability function[2]. This confirms the observations made by other authors[5,6], provided that the observation period is long enough (one month at least).

In a second step, long-term scintillation statistics are derived from the inferred refractive-index turbulence profiles, using theoretical results of wave propagation through a turbulent medium[7], with the classical hypotheses of well developed turbulence and weak scintillation[8]. Under the classical assumption of a log-normally distributed short-term scintillation variance σ_χ^2, the mean scintillation variance is expressed as:

$$\overline{\sigma_\chi^2} = 42.48 \frac{k^{7/6}}{(\sin\theta)^{11/6}} \sum_z \overline{< C_n^2(z) >} z^{5/6} \Delta z$$

where k is the free-space wave number, θ the elevation angle and $\overline{< C_n^2(z) >}$ represents the mean structure-function parameter, at height z above the ground and averaged over the period of available radiosonde data. This expression is asymptotically valid for

$$L_0 >> \sqrt{\lambda \frac{z}{\sin\theta}}$$

where L_0 is the outer scale of turbulence. The expression of the long-term variance of scintillation variance, σ^2, is more involved and can be found in Vasseur[2]. Assuming that the long term scintillation variance is log-normally distributed, i.e.

$$p\left(\sigma^2\right) = \frac{1}{\sqrt{2\pi}\sigma_\chi^2 s} \exp\left[-\frac{\left[\ln\left(\sigma_\chi^2/m\right) \right]^2}{2s^2} \right]$$

both m and s parameters are calculated from the mean and standard deviation of the scintillation variance, $\overline{\sigma_\chi^2}$ and $\sigma_{\sigma_\chi^2}^2$.

The following problem is however required to be solved. The C_n^2 profile is calculated by using the profiles of the potential temperature and the humidity, as well as their derivative, and the derivative of directional wind-speed. Taking the classical two-point

derivative procedure enhances the effect of the noise present in the measured radiosonde data. The refractive-index structure parameter can thereby present extremely high values caused by near zero-divisions. This significantly affects the prediction of *m* and *s* parameters and consequently, the cumulative statistics of scintillation. Filtering the input data versus height is not a viable solution, because it reduces the height resolution which is already poor.

A first step to alleviate the problem has been to use averaging of the derivatives. Various averaging lengths have been used and Fig. 1 shows the impact of the various choices on the final scintillation statistics versus measured data[2]. The final cumulative statistic curve is very sensitive to the averaging length. A further removal of unrealistic $< C_n^2 >$ values eventually provides good prediction accuracy. The criterion for the removal of those values is based on the log-normal behaviour of the long-term probability of the statistical distribution of $< C_n^2 >$ for a given height. In that case, the median value can be calculated from the mean and the standard deviation, using the relation

$$C_n^2\big|_{50} = \frac{\left\langle C_n^2 \right\rangle^2}{\sqrt{\sigma^2_{C_n^2} + \left\langle C_n^2 \right\rangle^2}}$$

and can be compared with the measured one. A discrepancy of more than 100% indicates non-valid values that are to be removed. This threshold value of 100% is however somehow arbitrary and may not be valid for all the radiosonde types and all the sites.

A better solution might be to rely on more elaborate derivation methods in order to blindly improve the quality and the accuracy of the prediction. As an example, a 4-point derivative has been used and yields a clear improvement as seen in Fig. 2. In this case, the method is fully automatic and there is no need to remove unrealistic $< C_n^2 >$ values. The only check to be performed is the verification for avoiding a zero divide in the calculation of $< C_n^2 >$.

2.2 Use of high resolution radiosoundings

The use of high resolution radiosoundings enhances the height resolution and should improve the accuracy of $< C_n^2 >$. The drawback is that the noise present in the measured data influences the $< C_n^2 >$ profile that becomes very noisy. So, further work has to be done in order to improve the situation. Furthermore, no measured scintillation statistics are available on the sites where high resolution radiosoundings are available. So, no direct verification can be performed, only a comparison between low-resolution and high-resolution radiosoundings can be performed. Figure 3 shows $< C_n^2 >$ calculated using the two types of radiosoundings and it shows a difference of roughly one order of magnitude of $< C_n^2 >$ between the two curves, taken at the same place and during the same time period! This effect has to be further analysed and is probably related to the preprocessing of the radiosonde data, which is different for both resolutions.

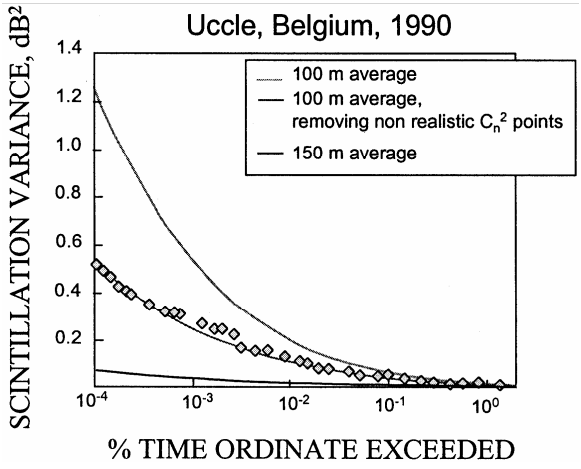

Fig. 1 — Predicted (with 2 different averaging and further removal of unrealistic C_n^2 values) and measured (◊) cumulative distribution of scintillation variance at 12.5 GHz

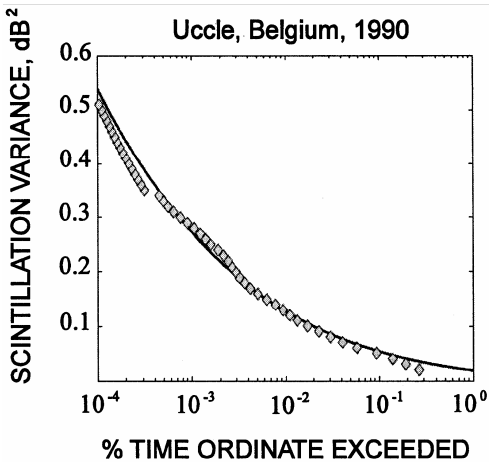

Fig. 2 — Predicted cumulative distribution of scintillation variance at 12.5 GHz, using a 4-point derivative, compared to measured (◊) cumulative distribution

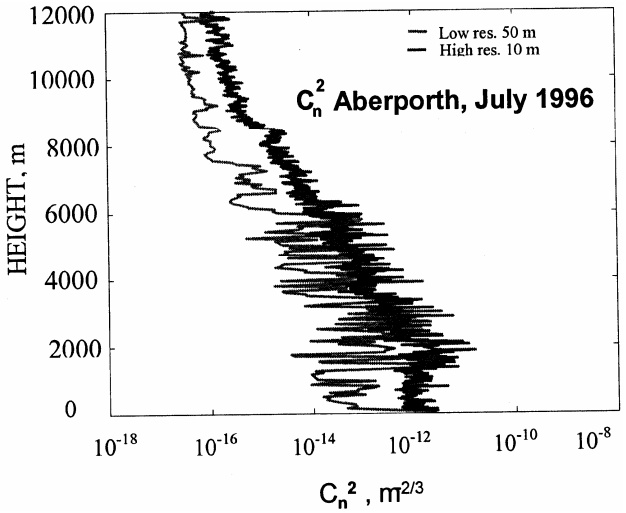

Fig. 3 — Comparison between height profiles of $<C_n^2>$ at Aberporth (UK), for July 1996, calculated using low-resolution (50 m interpolated) and high-resolution (10 m) radiosoundings

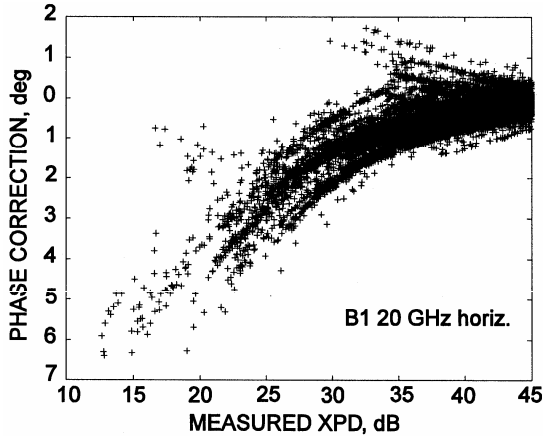

Fig. 4 — Phase imbalance between C_{ll} and C_{rr}

3 Depolarisation prediction

The full characterization of the troposphere as a depolarizing medium relies on the estimation of the transfer matrix for circular polarization, which is a 2 × 2 matrix relating the actual electric field vector with the vector which would be obtained in the absence of the atmospheric phenomena. If all polarization parameters are to be considered, a complete stochastic model can be obtained using the so-called "quasi-physical" parameters (anisotropy and canting angle). These parameters are strictly related to the physical mechanisms producing depolarisation (hydrometeor axes, turbulence, etc.) and can be predicted from climatic parameters, such as the ice content parameters[9-11].

If the double-polarization data are linearly-polarized, one must compute the circularly-polarized matrix. From the B_1 (19.7 GHz) switched beacon of the Olympus satellite measured data (matrix **M**, for local horizontal and vertical polarizations *h* and *v* at the earth receiver), one can first compute the corresponding matrix **T** along **x** and **y** polarizations as (τ is the tilt angle):

$$\mathbf{T} = \begin{bmatrix} \cos\tau & \sin\tau \\ \sin\tau & -\cos\tau \end{bmatrix} \times \mathbf{M} \times \begin{bmatrix} \cos\tau & \sin\tau \\ \sin\tau & -\cos\tau \end{bmatrix}$$

where

$$\mathbf{M} = \begin{bmatrix} M_{hh} & M_{hv} \\ M_{vh} & M_{vv} \end{bmatrix}$$

This matrix **T** is then converted into the circular polarisation (CP) transfer matrix **C**:

$$\mathbf{C} = \frac{1}{2}\begin{bmatrix} T_{xx} + T_{yy} + j(T_{yx} - T_{xy}) & T_{xx} - T_{yy} + j(T_{yx} + T_{xy}) \\ T_{xx} - T_{yy} - j(T_{yx} + T_{xy}) & T_{xx} + T_{yy} - j(T_{yx} - T_{xy}) \end{bmatrix}$$

Under very general assumptions (i.e. predominant forward scattering propagation, longitudinally homogeneous medium, particles' shape characterised by a symmetry axis) the diagonal elements of the transmission matrix in linear polarization should be equal. During the OLYMPUS and ITALSAT propagation campaigns it was observed that the measured values of C_{ll} and C_{rr} were not equal in phase, because $T_{yx} \neq T_{xy}$. This has been ascribed to a phase shift induced by the polarization switches in both the OLYMPUS and ITALSAT propagation payloads. Therefore, a phase correction is performed, so that $C_{ll} = C_{rr}$ with the phase equalling the average phase of rough C_{ll} and C_{rr}. Figure 4 illustrates the phase difference as a function of XPD level for all events in year 1990 at the receiving station of Lessive, in Belgium.

The matrices **T** and **M** are then re-computed after phase correction. This correction is not required for circularly polarized beacons, such as the Italsat 50 GHz beacon. Finally, the off-diagonal elements of the "reduced" circular polarization matrix can be estimated as:

$$\delta_{lr} = C_{lr}/C_{rr}$$
$$\delta_{rl} = C_{rl}/C_{ll}$$

The rain canting angle ϕ_{rain} is based on the circular depolarisation measured data. In order to derive the

complex rain anisotropy from the data, the theoretical calculation of rain anisotropy for perfect alignment of the rain drops (with unitary reduction factor) is estimated, assuming the MP drops size distribution. Finally, the actual rain reduction factor is inferred from the "measured" anisotropy. The ice content is derived assuming ice crystals are needles. The canting angle and anisotropy are estimated, based on the phase of rain anisotropy (χ_{rain}) and the circular depolarisation measured data[12]. Assuming on a first approximation that the particles located in the melting layer are less effective than rain and ice particles in depolarizing at this frequency, the total XPD can be finally estimated based on the assumption of a cascaded medium:

$$\mathbf{T} = \mathbf{T}_{rain} \times \mathbf{T}_{ice}$$

Both matrices are calculated from the previously estimated parameters. Figure 5 shows the measured and simulated data calculated using the above described method. The simulated data follow quite accurately the measured XPD/CPA data, which proves that the hypotheses made (ice and rain separated, two layers model, needles shape for ice, …) are realistic. This method allows the simulation of XPD/CPA instantaneous values for other frequencies and elevation angles. It is also possible to retrieve the ice content and to calculate its statistics.

The physical parameters of rain and ice are extracted from the measured transmission matrix at 20 GHz, using the Olympus B2 satellite measurements. The XPD-CPA graph can then be reconstructed at any other frequency. A comparison between reconstructed and measured XPD-CPA at 40 GHz (Italsat), is shown in Fig. 6. The 40 GHz XPD (crosses), reconstructed from 50 GHz dual polarisation measurements, agrees quite well with the measurements (dots). A small constant difference in level between simulation and measurement can be observed. This is due to the fact that at 40 GHz, which was a single polarised beacon, the template extraction could only be performed using depolarisation vectors and not the full transmission matrix (like for the dual polarization beacon at 50 GHz). In this case eventual differential gains between orthogonal polarization in the transmitter and receiver RF cannot be removed only by vector correction, whereas matrix correction and comparison with frequency scaled measurements can identify and correct this effect.

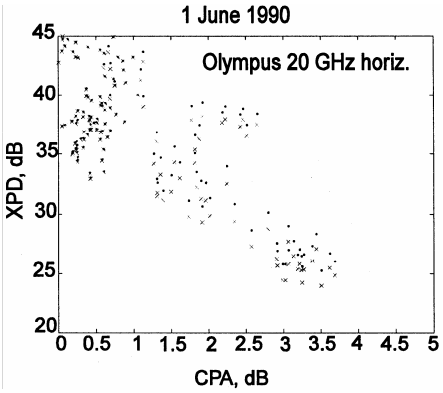

Fig. 5 — 1st June, 1990 results at 19.7 GHz, cross-polar discrimination (XPD) versus copolar attenuation (CPA), horizontal polarization; measured data (·) and simulations (x)

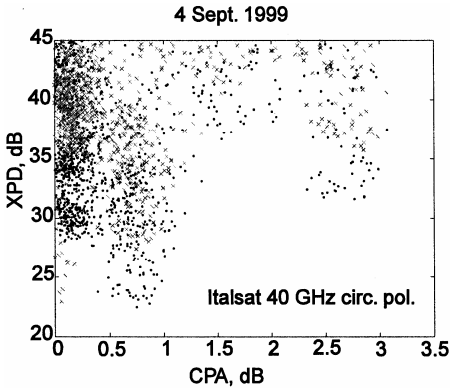

Fig. 6 — Measured (.) and simulated (x) data for the rain event of 4 Sep. 1999, at 40 GHz, circular polarization (CP)

4 Conclusions

Two methods have been presented, improving the prediction of scintillation variance and depolarisation statistics. Their accuracy is good but they show some weaknesses; further developments are needed. Radiosoundings have proved their interest for the calculation of scintillation statistics all over the world. The method presently used for the prediction shows however a high sensitivity to the raw data properties and pre-processing, and should be improved. These methods have to be further tested on a larger number of events and at various locations.

Acknowledgements

This work was partially carried out in the framework of an ESA/ESTEC Contract 17841-04 entitled "Characterization and modelling of propagation effects in the 20-50 GHz band". UCL is grateful to Dipartimento di Elettronica e Informazione-IEIIT/CNR, Politecnico di Milano for the processed Italsat data.

References

1 ITU-R Recommendation P.618-8, *Recommendations of the ITU, International Telecommunications Union*, ITU-R, 2003.

2 Vasseur H, Prediction of tropospheric scintillation on satellite links from radiosonde data, *IEEE Trans Antennas Propag (USA),* 47 (1999) 293.

3 Van Zandt T E, Gage K S, Warnock J M, An improved model for the calculation of profiles of C_n^2 and ε in the free atmosphere from background profiles of wind, temperature and humidity, *20th Conf. on Radar Meteor,* Nov. 30-Dec. 3, Boston (USA), Am. Met. Soc, 129 (1981).

4 Warnock J M, Van Zandt T E, Green J L, A statistical model to estimate mean values of parameters of turbulence in free atmosphere, *7th Symposium on Turbulence and Diffusion,* Nov. 12-15, Boulder, Co (USA), Am Met Soc, 1985.

5 Hufnagel R E, *Variations of atmospheric turbulence*, Dig Tech Papers, Tropical Meet. Opt. Propag Turbulence, Washington DC, USA, pp. wal.1-4 (1974).

6 Chadwick R B, Moran K P, Long-term measurements of C_n^2 in the boundary layer, *Radio Sci (USA)*, 15 (1980) 355.

7 Tatarskii V I, *The effects of the turbulent atmosphere on wave propagation*, Translated from Russian, Israel Program for Scientific Translation, Jerusalem, 1971.

8 Ishimaru A, *Wave propagation and scattering in random media*, vol.2, (Academic Press, New York), 1978.

9 Martellucci M & Paraboni A, *Measurements and modelling of rain and ice depolarization on spatial links in the Ka and V band frequency bands,* Millennium Conference on Antennas and Propagation AP 2000, CD-ROM, 2000.

10 Martellucci A, Poiares Baptista J P V & Blarzino G, *New climatological databases for ice depolarization on satellite radio links*, COST 280 1st International Workshop on Propagation Impairment Mitigation for Millimetre Wave Radio Systems, 2002.

11 Van de Kamp M M J L, *Climatic radiowave propagation models for the design of satellite communication systems*, PhD thesis, (T U Eindhoven, The Netherlands), 1999.

12 Amaya C & Vanhoenacker-Janvier D, Estimation of the effective ice content on earth-satellite paths from dual-polarisation measurements at Ka-band, *IEE Proc Microwave Antennas Propag (UK)*, 147 (2000) 315.